INTERPRETATION OF MAGNETIC ANOMALIES BY POWER SPECTRUM ANALYSIS

A. MESKÓ and K. KIS

Department of Geophysics, Eötvös University, Budapest

Received: 1 Juli 1978

SUMMARY

Power spectra of magnetic field data have been used to estimate the average depth and some other parameters of magnetized bodies. In this paper, which consitutes Part I of a series, the foundations and applicability of the method are discussed in some details. The logarithms of the radial spectra due to prismatic bodies are investigated. It is shown that although the dominating term in the spectra is the term $-4\pi h_{top} f_r$, connected with the depth to the top of the magnetized bodies the influence of other parameters and their probability density functions can not be neglected.

The contribution of a deeper ensemble of prismatic bodies dissappears very rapidly with increasing f_r thus in the estimation of the average depth to the top of deeper sources the first few spectral lines may be used, only. The depth extent could be determined very seldom even for the shallower ensemble of sources.

Introduction

Spectral analysis of potential field data has become a standard tool for geophysical interpretation in recent years. Frequency spectra of the gravity and magnetic fields have been derived for a number of geometrical bodies and for various distribution of certain types of bodies including two- and three-dimensional dykes, two-dimensional structures with polygonal cross sections, random distributions of sources in a given depth interval, monopole and dipole coating in equivalent strata etc. (Odegard and Berg, 1965, Bhattacharyya 1965, 1966, 1971, Spector and Bhattacharyya, 1966, Spector and Grant, 1970, Syberg, 1972, Bhattacharyya and Leu, 1975, Sengupta and Dar, 1977 and others).

It has been found that the expressions of the spectra, besides other factors, consist of sums of exponentials with exponents which are linear functions of frequency. Therefore when plotted in a logarithmic scale the amplitude spectra or power spectra show frequency intervals, where the functions may well be approximated by straight lines. The slopes of these lines can be used to estimate certain characteristic parameters of the bodies (depths to the top of the prismatic bodies, or depths of the equivalent strata or depths to the bottom etc).

Analysis of measured gravity and magnetic field data have shown that the theoretical foundations are sound. Power spectra almost always indicate two distinct depths which may be related to a set of deeper and a set of shallow sources. In some cases the depth extent of one set of sources can also be estimated (Spector and Grant 1970, Naidu, 1970, Lehmann, 1970, Syberg, 1972, Bhattacharyya and Leu, 1975, Cianciara and Marcak, 1976, Hahn, Kind and Mishra, 1976). Though the good separation of sources at different depths, especially in the case of the gravity anomalies, needs a more satisfactory explanation than the one what the present theory provides, the method could be considered as well established in current practice.

The scope of this paper is to discuss the application and results of the method to vertical component anomalies of the magnetic field in the Pannonian Basin. Some of the preliminary results have been shortly summarized elsewhere (Meskó and Kis, 1977). In Part I we discuss the underlying principles of the method and report investigations by prismatic models.

Power spectrum of the magnetic field due to a vertical prismatic body

The vertical prism has been considered as the basic interpretational model of magnetic field components. This simple model has been used with success for estimating varicus parameters of the magnetized bodies from the magnetic anomalies (Peters, 1949, Vacquier, 1951, Steenland, 1962, etc). Spector and Grant (1970) attribute the success to the fact that magnetic anomaly patterns are largely shaped by the depths and horizontal dimensions of the sources besides the directions of their magnetization and they are influenced relatively little by the details of their boundaries. Thus we consider first the power spectrum of the magnetic anomalies due to single vertical prismatic bodies.

The expressions for the magnetic field vector components due to a vertical prismatic body as well as the corresponding Fourier spectra can be found in the literature (e. g. in Bhattacharyya, 1966). A general formula of the Fourier spectra including all cases of interest reads as

$$G(f_x,\ f_y) = \frac{2ab}{f_r}\,\mathrm{sinc}\,(af_x)\,\mathrm{sinc}\,(bf_y)(e^{-2\pi h_1 f_r} - e^{-2\pi h_2 f_r})\cdot I \qquad (1)$$

The factor I depends on several variables and it is related to the type of the anomaly field considered. When g(x, y) describes total magnetic field anomalies the factor I becomes

$$I = \frac{\pi m_0}{f_r}\,[-lLf_x^2 - mMf_y^2 + nNf_r^2 - \alpha_{12}f_xf_y + j\alpha_{13}f_xf_r + j\alpha_{23}f_yf_r]\cdot \qquad (2)$$

The variables in the formulas denote the following quantities

a	width of the body,
b	length of the body,
h_1	depth to the top of the body,
h_2	depth to the bottom of the body,
m_0	intensity of magnetization within the body,
L, M, N	direction cosines of magnetization,
l, m, n	direction cosines of the geomagnetic field,
f_x and f_y	spatial frequencies (or wavenumbers) in the x and y directions, respectively,

$f_r = (f_x^2 + f_y^2)^{1/2}$ radial spatial frequency.
The notations are explained in *Fig. 1.*

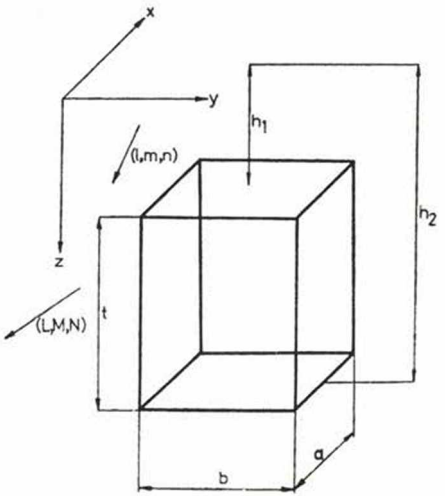

Fig 1. Notations used in the expressions describing the magnetic fields due to prismatic bodies

The functions α_{12}, α_{13} and α_{23} are defined by

$$\alpha_{12} = Lm + Ml, \tag{3.a}$$

$$\alpha_{13} = Ln + Nl, \tag{3.b}$$

$$\alpha_{23} = Mn + Nm. \tag{3.c}$$

When the body is magnetized in the direction of the geomagnetic field

$$l = L, \quad m = M, \qquad n = N$$

and the formulas (3) become

$$\alpha_{12} = 2\ \mathrm{lm}, \tag{4.a}$$

$$\alpha_{13} = 2\ \mathrm{ln}, \tag{4.b}$$

$$\alpha_{23} = 2\ \mathrm{mn}. \tag{4.c}$$

When we consider vertical anomalies $l = m = 0$ and the factor I becomes

$$I = \frac{\pi m_0}{f_r}\left[Nf_r^2 + jLf_x f_r + jMf_y f_r\right]. \tag{5}$$

The power spectrum can be derived by taking the squared modulus of the spectrum $G(f_x, f_y)$. Let us introduce polar coordinates in the frequency domain by $f_x = f_r \cos\alpha$, $f_y = f_r \sin\alpha$. Then we may write for the general case

$$|G(f_r, \alpha)|^2 \equiv E(f_r, \alpha) = KS^2(f_r, \alpha)\, R_T^2(\alpha)\, e^{-4\pi h_1 f_r}\,(1 - e^{-2\pi t f_r})^2, \tag{6}$$

with

$$K = (2\pi)^2 a^2 b^2 m_0^2,$$

$$S^2(f_r, \alpha) = \mathrm{sinc}^2(af_r \cos\alpha)\,\mathrm{sinc}^2(bf_r \sin\alpha),$$

$$R_T^2(\alpha) = n^2 + (l\cos\alpha + m\sin\alpha)^2,$$

$$R_M^2(\alpha) = N^2 + (L\cos\alpha + M\sin\alpha)^2,$$

$$t = h_2 - h_1 \ (\text{depth extent}).$$

The special cases, mentioned previously, are obtained by the following substitutions

$$R_T^2(\alpha) = R_M^2(\alpha)$$

(induced magnetization),

$$R_T^2(\alpha) = 1.$$

(vertical component of the magnetic field).

The radial power spectrum is obtained by integrating over the variable α, and it has an even simpler shape as follows

$$E(f_r) = K_r\, S_t^2(f_r)\, e^{-4\pi h f_r}\,(1 - e^{-2\pi t f_r})^2 \tag{7}$$

where

$$K_r = \frac{1}{2\pi}\int_0^{2\pi} K R_T^2(\alpha)\, R_M^2(\alpha)\, d\alpha, \tag{8}$$

$$S_r^2(f_r) = \frac{1}{2\pi}\int_0^{2\pi} S^2(f_r, \alpha)\, d\alpha = \frac{1}{2\pi}\int_0^{2\pi} \mathrm{sinc}^2(af_r\cos\alpha)\,\mathrm{sinc}^2(bf_r\sin\alpha)\, d\alpha, \tag{9}$$

and $h = h_1$.

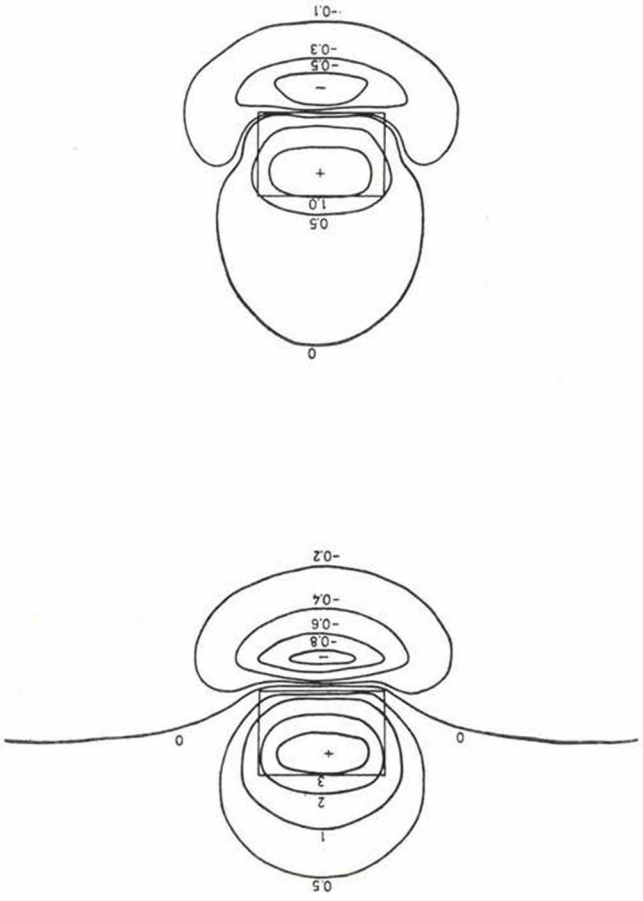

Fig. 2. Total magnetic field due to rectangular prisms with parameters
$a = 4, b = 6, h = 1, t = \infty$ (top) and
$a = 4, b = 6, h = 1, t = 1$ (bottom)
(induced magnetization is assumed in both cases, the geomagnetic field vector has inclination $I = 60°$, declination $D = 0°$)

The logarithm of the radial power spectrum than becomes

$$\ln E(f_r) = K + 2 \ln S_r(f_r) + 2 \ln(1 - e^{-2\pi t f_r}) - 4\pi h f_r. \qquad (10)$$

The dominating term is the linear function $-4\pi h f_r$ though $\ln S_r (f_r)$ and $\ln (1\text{-}\exp(\text{-}2\pi t f_r))$ may also modify the rate of linear decrease with increasing f_r. The extent of the effect of these factors have been investigated by numerical models.

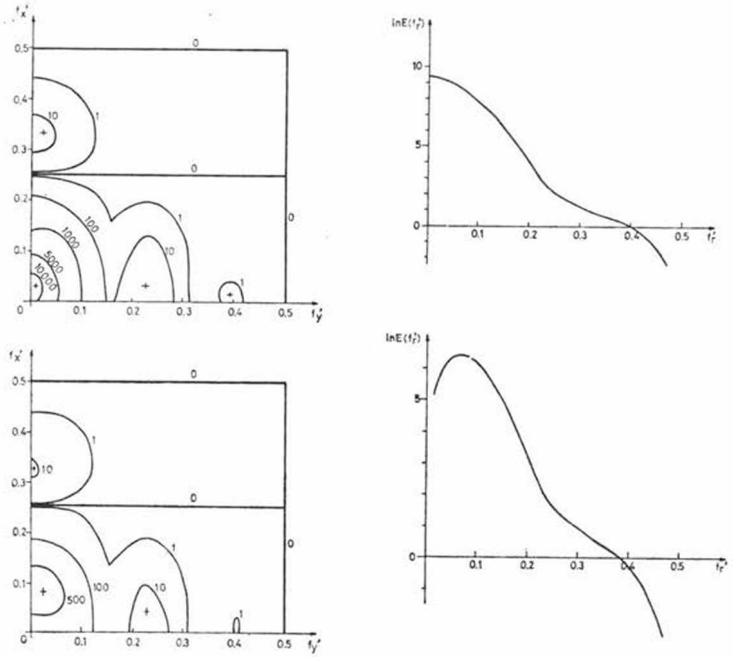

Fig 3. Two-dimensional spectra (on the left) and logarithmic radial spectra (on the right) of the magnetic field data shown in Fig. 2.

Investigations of the logarithmic power spectra due to prismatic bodies

In order to imitate the processing of real data as close as possible we computed the magnetic fields due to various prismatic bodies in 32×32 points forming a regular square grid. The origin of the coordinate axis x and y was placed above the center of the prism. The fourier transforms of the data have been determined by the FFT (Fast Fourier Transform) algorithm and radial power spectra have been derived by numerical integration of the squared modulus of the Fourier transforms. Data windows have not been applied.

Fig. 2. shows two examples of the computed magnetic anomaly due to prisms with parameters $a = 4$, $b = 6$, $h = 1$, $t = \infty$ and $a = 4$, $b = 6$, $h = 1$, $t = 1$ (dimensions are understood in the units of grid spacing) and with inclination 60°, declination 0°, induced magnetization in both cases. Computed data have been compared to magnetic fields for the same models published in the literature (Andreasen and Zietz, 1969) in order to estimate the accuracy of our method based on the Fourier transform approach. The two-dimensional Fourier transforms of the previous examples are given in *Fig. 3* together with the logarithmic power spectrum (on the right).

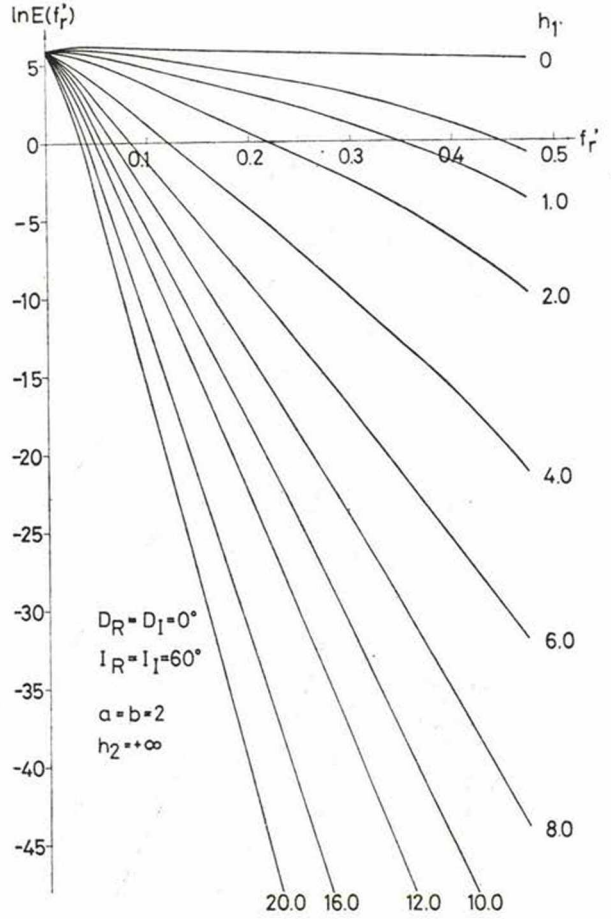

Fig. 4. Logarithmic radial spectra of magnetic fields (total field) due to prisms illustrating the effect of depth to the top of the bodies. Parameters are indicated. Map window is 32×32

Figures 4 – 10 show some of the results of model investigations.

Figure 4 illustrates the logarithmic spectra for prisms and shows the effect of the depth to the top of the prism. The horizontal dimensions are $a = b = 2$ the vertical extents are infinite and the depths to the top are equal to 0, 0.5, 1, 2, 4, 6, 8, 10, 12, 16 and 20. (All dimensions are expressed in units of grid spacing.) *Fig. 5* shows the logarithmic spectra for prisms with the same horizontal cross section (2×2) but for $h_2 = 20$ and $h_1 = 0$, 0.5, 1, 2, 4, 6, 8, 10, 14 and 18.

These figures proves that the effect of the depths to the top dominates at least for cases when the horizontal cross section is small enough compared to the dimensions of the map window (2×2 compared to 32×32).

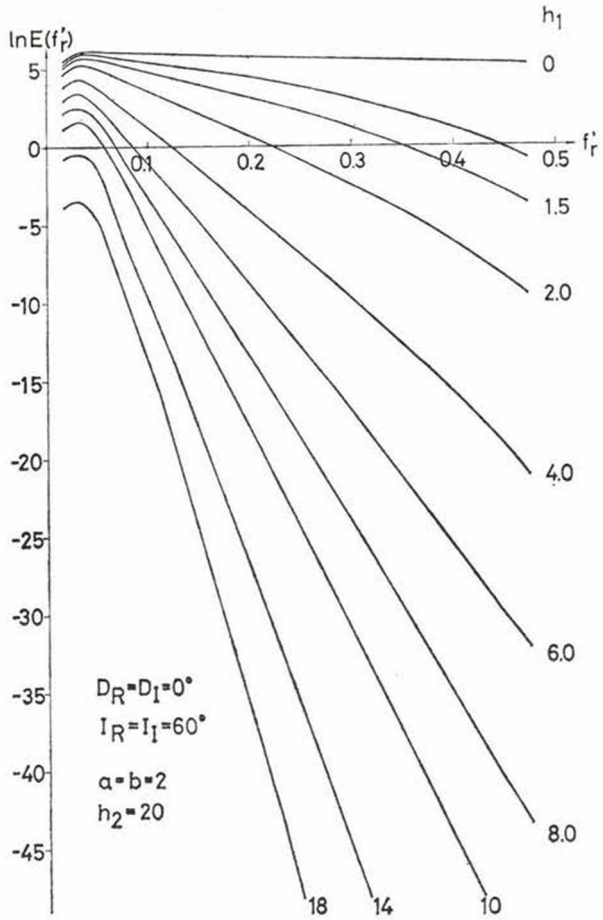

Fig. 5. Logarithmic radial spectra of magnetic fields (total filed) due to prisms, illustrating the effect of depth to the top of the bodies. Parameters are indicated. Map window is 32×32

The disturbing effects of larger horizontal dimensions could be evaluated by *Figs. 6 and 7*.

In *Fig. 6* logarithmic power spectra due to vertically infinite prisms with tops at 2 grid units are shown for various horizontal cross sections $a = b = 0.5, 1, 2, 4, 6, 8$ and 10. *Fig. 7* depicts logarithmic spectra for the same parameters except that now bottom is at 20 grid units. Doubled dashed lines in both figures indicate the direction of the linear term $-4\pi h f_r$. As it can be seen the increasing horizontal size tapers the spectra toward higher wavenumbers, i. e. it makes the slope steeper. Thus depth estimates derived from logarithmic spectra of bodies with large horizontal dimensions (large is understood again as compared to the size of the map) are too large. The influence, however, does not seen serious until $a \leq 2$.

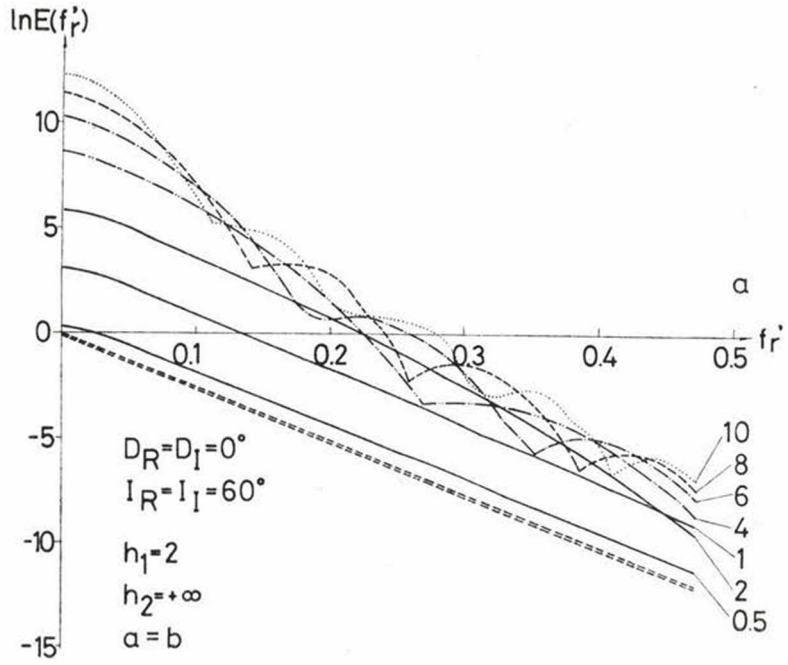

Fig. 6. Logarithmic radial spectra of magnetic fields (total field) due to prisms, illustrating the effect of horizontal dimensions. Numbers at the end of the curves indicate the values a = b. Doubled dashed line shows the dominating term $-4\pi h_1 f_r$

The effect of the depth extent is appreciable only, when both h and $t = h_2 - h_1$ are small. Let us consider the last two factors in equation (7),

$$g(h, t, f_r) = e^{-4\pi h f_r}(1 - e^{-2\pi t f_r})^2.$$

The product has a maximum, where

$$\frac{\partial g}{\partial f_r} = 0$$

which leads to the equation

$$2\pi t f_r = \ln\left(\frac{t}{h} + 1\right)$$

and it gives for the position of the maximum

$$(f_r)_{\max} = \frac{1}{2\pi t} \ln\left(\frac{t}{h} + 1\right). \tag{10}$$

The radial power spectrum and correspondingly the logarithmic power spectrum may posess a maximum. *Table 1* summarizes the $(f_r)_{\max}$ for some values of the parameters t and h. When t is small enough the combined effect

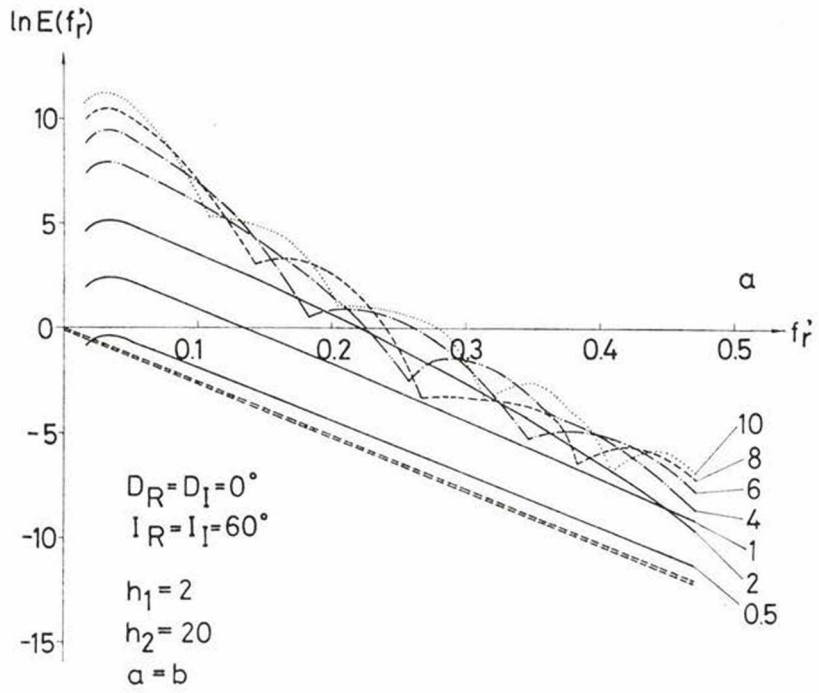

Fig. 7. Logarithmic radial spectra of magnetic fields (total field) due to prisms, illustrating the effect of horizontal dimensions. Numbers at the end of the curves indicate the values $a = b$. Doubled dashed line shows the dominating term $-4\pi h_1 f_r$

of t and h gives a pronounced peak in the logarithmic spectrum. With increasing t, however, the peak shifts toward smaller frequencies. We always deal with a finite number of data therefore when t becomes large the maximum can not be seen at all. The spectrum lines are at $(k/n;\ 1/M)$ $k = 0, \pm 1, \pm 2, \ldots, N/2$, $l = 0, \pm 1, \pm 2, \ldots, \pm M/2$ where N and M denote the dimensions of the map given in grid units therefore $(f_r)_{max} \cdot \min(1/N, 1/M)$ can not be seen. In *Table 1* (lower part) we also give the smallest $(f_r)_{max}$ which possibly can be detected for some reasonable number of data.

Finite vertical size is illustrated by *Figures 8, 9 and 10* for some realistic values of the parameters.

In *Fig. 8* $t = 0.1$ and $h_1 = 0, 0.5, 1.5, 2.0, 2.5, 4, 6$ and 8. In *Fig. 9* $t = 0.4$ and $h = 0, 0.5, 1.0, 1.5, 2.0, 2.5, 3, 3.5, 4$ and in *Fig. 10* $t = 1.0$, and $h = 0, 0.2, 0.4, 0.6, 0.8, 1.0, 1.2, 1.4, \ldots, 3.0$. The horizontal dimensions are for all the depicted cases $a = b = 2$.

The places of the maxima computed from (10) and observed in the logarithmic spectra can be compared in *Table 2*.

Table 1.

The position of the spectral peak $(f_r)_{max}$ for some values of 5 (depth of the top) and t (depth extent) 5 and t are given in km, f_r in $(km)^{-1}$ units

h / t	0.1	0.2	0.5	1.0	2.0	3.0	4.0	5.0	10.0
0.1	1.103	.645	.290	.152	.0776	.0522	.0393	.0315	.0158
0.2	.874	.552	.268	.145	.0758	.0514	.0388	.0312	.0158
0.25	.789	.516	.258	.142	.0750	.0510	.0386	.0311	.0157
0.3	.735	.486	.249	.139	.0741	.0506	.0384	.0309	.0157
0.4	.640	.437	.234	.134	.0725	.0498	.0397	.0306	.0156
0.5	.570	.399	.221	.129	.0710	.0491	.0375	.0303	.0155
0,75	.454	.331	.194	.119	.0676	.0474	.0365	.0297	.0153
1.0	.382	.285	.175	.110	.0645	.0458	.0355	.0290	.0152
2.0	.272	.191	.128	.087	.0586	.0460	.0323	.0268	.0145
3.0	.182	.147	.103	.074	.0486	.0368	.0297	.0249	.0139
4.0	.148	.121	.087	.064	.0437	.0337	.0267	.0234	.0134
5.0	.125	.104	.076	.057	.0399	.0312	.0258	.0221	.0129
6.0	.109	.091	.068	.052	.0368	.0291	.0243	.0209	.0125
7.0	.097	.081	.062	.047	.0324	.0274	.0230	.0199	.0121
8.0	.087	.074	.056	.044	.0320	.0258	.0219	.0190	.0117
9.0	.080	.068	.052	.041	.0310	.0245	.0208	.0182	.0114
10.0	.073	.063	.048	.038	.0285	.0233	.0199	.0175	.0110
15.0	.053	.046	.036	.029	.0227	.0190	.0165	.0147	.0097
20.0	.042	.037	.303	.024	.0191	.0162	.0143	.0128	.0087
25.0	.035	.031	.025	.021	.0166	.0142	.0126	.0114	.0080
30.0	.030	.027	.022	.018	.0147	.0127	.0114	.0103	.0074

The smallest $(f_r)_{max}$ (in km^{-1}) which can be detected when number of data is $N \times N$ and grid spacing is s

s / N	0.5 km	1 km	2 km	5 km	10 km
16	0.1250	0.0625	0.0313	0.0125	0.0063
32	0.0625	0.0313	0.0156	0.0063	0.0031
48	0.0417	0.0283	0.0104	0.0042	0.0021
64	0.0313	0.0156	0.0078	0.0031	0.0016
128	0.0156	0.0078	0.0039	0.0016	0.0008
256	0.0078	0.0099	0.0020	0.0008	0.0004

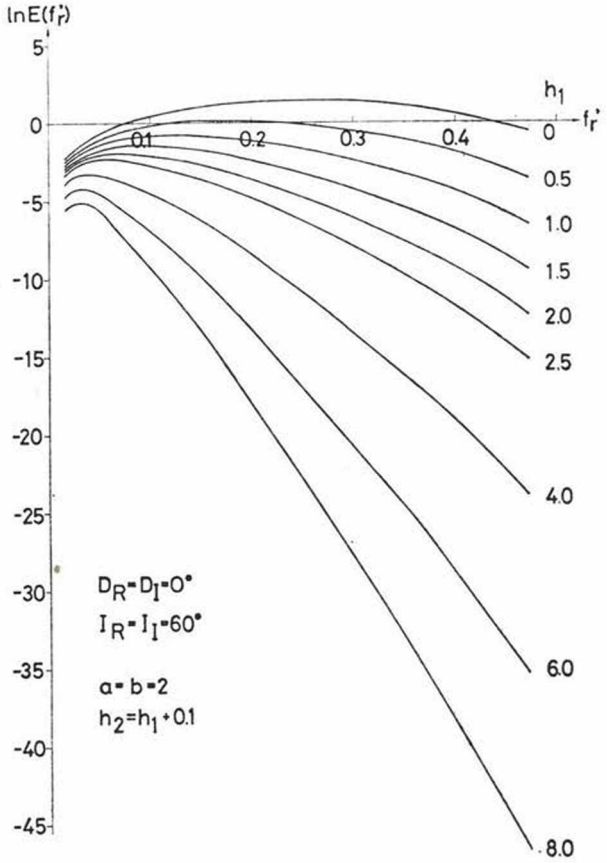

Fig. 8. Logarithmic radial spectra illustrating the effect of finite vertical size, $t = 0.1$ i.e. all cases correspond to very thin layers. Other parameters are indicated

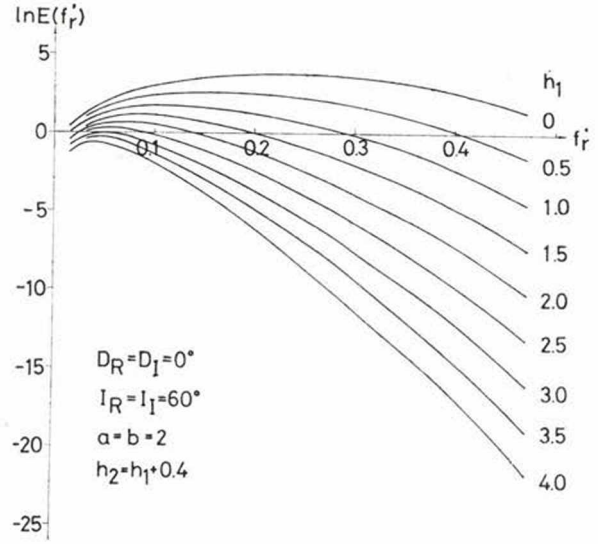

Fig. 9. Logarithmic radial spectra illustrating the effect of finite vertical size. $t = 0.4$, other parameters are indicated

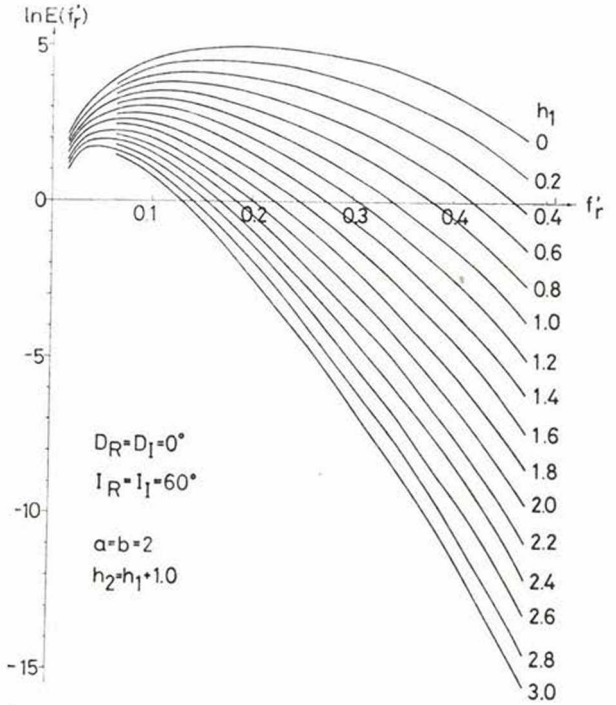

Fig. 10. Logarithmic radial spectra illustrating the effect of finite vertical size, $t = 1.0$, other parameters are indicated

Table II.

Position of the spectral peak computed from the approximation of Eq(10) compared to the position of spectral peaks in the spectra of model bodies. The spectra ln $E(f_r')$ are shown in Figs. 8, 9 and 10 respectively

$a = b = 2$ h_1	$t = 0.1$ h_2	approximate $(f_r')_{max}$ (Eq. 10)	model
0.5	0.6	0.2902	0.1717
1.0	1.1	0.1517	0.1231
1.5	1.6	0.1027	0.0934
2.0	2.1	0.0777	0.0717
2.5	2.6	0.0624	0.0629
4.0	4.1	0.0393	0.0371

$a = b = 2$ h_1	$t = 0.4$ h_2	approximate $(f_r')_{max}$ (Eq. 10)	model
0.5	0.9	0.2339	0.1562
1.0	1.4	0.1339	0.1125
1.5	1.9	0.0941	0.0872
2.0	2.4	0.0725	0.0645
2.5	2.9	0.0591	0.0605
3.0	3.4	0.0498	0.0468
3.5	3.9	0.0431	0.0380
4.0	4.4	0.0379	0.0269

$a = b = 2$ h_1	$t = 1$ h_2	approximate $(f_r')_{max}$ (Eq. 10)	model
0.2	1.2	0.2852	0.1630
0.4	1.4	0.1994	0.1404
0.6	1.6	0.1561	0.1240
0.8	1.8	0.1291	0.1031
1.0	2.0	0.1103	0.0973
1.2	2.2	0.0965	0.0890
1.4	2.4	0.0858	0.0791
1.6	2.6	0.0773	0.0706
1.8	2.8	0.0703	0.0673
2.0	3.0	0.0645	0.0642
3.0	4.0	0.0458	0.0387

Power density spectra of randomly distributed prisms

Let us consider now the power spectrum of several prismatic bodies. The Fourier spectrum of the magnetic field due to the bodies is

$$G(f_x,\ f_y) = \sum_{i=1}^{n} G_i(f_x,\ f_y)\, e^{-j2\pi(f_x x_i + f_y y_i)}$$

where $G_i(f_x, f_y)$ denotes the spectrum of the ith prism and $(x_i,\ y_i)$ denotes the center of the ith prism (n is the number of prisms).

The power spectrum as the squared modulus of $G_i(f_x, f_y)$ becomes

$$E(f_x, f_y) = |G(f_x, f_y)|^2 = \sum_{i=1}^{n} |G_i(f_x, f_y)|^2 + \sum_{i=1}^{n} \sum_{\substack{k=1 \\ i \neq k}}^{n} H_i^r(f_x,\ f_y)\, H_k^n(f_x,\ f_y) +$$

$$+ \sum_{i=1}^{n} \sum_{\substack{k=1 \\ i \neq k}}^{n} H_i^{im}(f_x,\ f_y)\, H_i^{im}(f_x,\ f_y)$$

where $H_i^r(f_x, f_y)$ and $H_i^{im}(f_x, f_y)$ are abbreviations for

$$H_i^r(f_x, f_y) = G_i^r(f_x,\ f_y) \cos 2\pi(f_x x_i + f_y y_i) + G_i^{im}(f_x,\ f_y) \sin 2\pi(f_x x_i + f_y y_i)$$

and

$$H_i^{im}(f_x, f_y) = -G_i^r(f_x, f_y) \sin 2\pi(f_x x_i + f_y y_i) + G_i^{im}(f_x, f_y) \cos 2\pi(f_x x_i + f_y y_i).$$

If the centers $(x_i,\ y_i)$ are randomly distributed the cross-products cancel each other or at least their contribution becomes negligibly small compared to the dominating term, i. e. compared to the sum of the power spectra due to individual prisms. This assumption fails when the number of prisms is small or there is some regularity in their distribution. Keeping this restriction in mind we proceed with the (approximate) equation

$$E(f_r) = \sum_{i=1}^{n} E_i(f_r) \equiv \sum_{i=1}^{n} E(a_i,\ b_i,\ h_i,\ t_i,\ f_r). \tag{11}$$

Let us assume next that the parameters of the prisms are not arbitrary but follow some probability distribution. The sum may be replaced by the ensemble average multiplied by the number of prisms. The ensemble average, in turn, can be evaluated if we assume that the parameters are independent and we assign to each of them some probability distribution.

The joint probability density function, including all parameters becomes a product of probability density functions each containing one parameter, only

$$Pr(a,\ b,\ t,\ h,\ \ldots) = Pr(a)\, Pr(b)\, Pr(t)\, Pr(h)\ \ldots$$

when the parameters are independent.

A further assumption may be that the average values of the inclination and the declination of the magnetic moment vector, do not differ significantly from the inclination and declination of the geomagnetic field. It involves that magnetization is essentially induced. This can be verified by the shape of individual anomalies. When the assumption seems to be justified we can write for the expected values

$$\mathcal{E}\{R_T^2(\alpha)\} = \mathcal{E}\{R_M^2(\alpha)\}.$$

The probability distribution of the other parameters can not be deduced from the data and various assumptions have to be made concerning the shape of the distributions.

E. g. Spector and Grant (1970) assumed uniform distributions for all parameters. Other distributions e. g. Gaussian distribution may also be used.

The expected value of the power density spectrum becomes

$$\mathcal{E}\{E(f_r, \alpha)\} = \int \ldots \int E(f_r, \alpha)\, Pr(a)\, Pr(b) \quad da\, db \ldots$$

Due to the simple structure of the assumed joint probability distribution the multiple integral can be factored into a product of integrals, each containing the contributions of some characteristic parameters

$$\mathcal{E}\{E(f_r\, \alpha)\} = 4\pi^2\, \bar{k}\, \mathcal{E}\{e^{-4\pi h f_r}\} \cdot \mathcal{E}\{(1 - e^{-2\pi t f_r})^2\} \cdot$$
$$\cdot\, \mathcal{E}\{S^2(f_r, \alpha)\}\, \mathcal{E}\{R_T^4(\alpha)\}. \tag{12}$$

where $\bar{k}$ denotes the expected value of abm_0.

When we take the radial power spectra by averaging over the variable α the last term becomes a constant factor. After taking the logarithm the constant factors become additive constants having no bearing upon the shape of $S(f_r)$. Three terms remain containing the effects of depth, depth extent and horizontal sizes, respectively. Each term will be discussed separately.

The influence of the depth (to the top of the prism)

Assuming first that h is uniformly distributed in the interval $(\bar{h} - \Delta h, \bar{h} + \Delta h)$ the expected value is obtained as follows

$$\mathcal{E}\{e^{-4\pi h f_r}\} = \frac{1}{2\Delta h} \int_{\bar{h}+\Delta h}^{\bar{h}-\Delta h} e^{-4\pi h f_r}\, dh = \frac{1}{2\Delta h} \left[\frac{e^{-4\pi h f_r}}{-4\pi f_r} \right]_{\bar{h}-\Delta h}^{\bar{h}+\Delta h} =$$

$$= e^{-4\pi \bar{h} f_r} \frac{sh(4\pi f_r\, \Delta h)}{4\pi f_r\, \Delta h}. \tag{13}$$

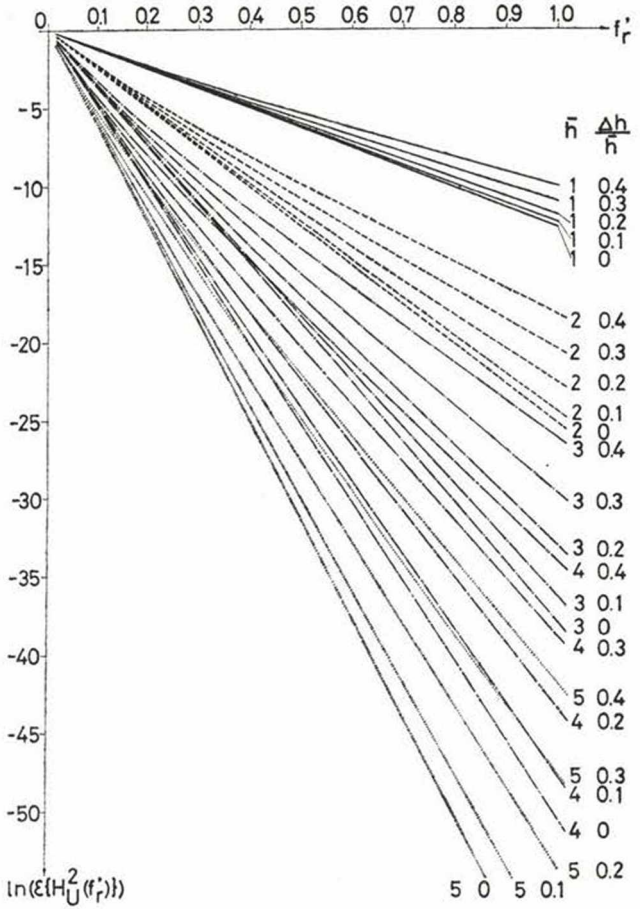

Fig. 11. The expected value of the dominating term $(-4\pi h f_r)$ if h follows a uniform distribution with expected value h and length Δh

The first factor dominate when $4\,\pi f_r\,\Delta h$ is sufficiently small. The effect of the length of the distribution can be estimated from *Fig. 11* which shows the logarithm of (13) for the average depths $\bar{h} = 1, 2, \ldots, 5$ and relative lengths $(\Delta h/\bar{h})$ of the uniform distribution $\Delta h/\bar{h} = 0.0,\ 0.1,\ 0.2,\ 0.3$ and 0.4.

Let us assume next that the probability of h is Gaussin with the parameters $(\bar{h}, \sigma)$. The expected value of the factor $\exp(-4\,\pi h f_r)$ then becomes

$$\mathcal{E}\{e^{-4\pi h f_r}\} = \frac{1}{\sqrt{2\pi}\,\sigma} \int_{-\infty}^{+\infty} e^{-4\pi h f_r}\, e^{-(h-\bar{h})^2/2\sigma^2}\, dh = e^{-4\pi \bar{h} f_r + 8\pi^2 \sigma^2 f_r^2}. \qquad (14)$$

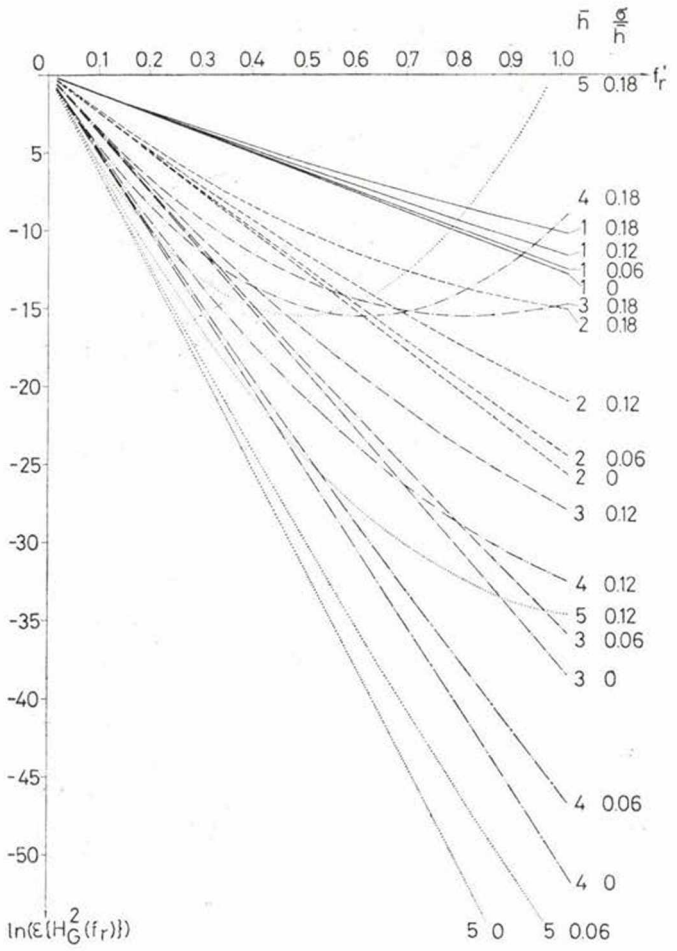

Fig. 12. The expected value of the dominating term $(-4\pi h f_r)$ if h follows a normal distribution with expected value h and standard deviation σ

The logarithm of the expected value contains now a parabolically increasing term $8\pi^2\sigma^2 f_r^2$ besides the linearly decreasing $-4\pi\bar{h}f_r$. Its effect is, again, negligible until σ remains sufficiently small. *Fig. 12* shows the logarithm of the expected value of $\exp[-4\pi f_r h]$ for some values of the parameters $\bar{h}$ and $\sigma/\bar{h}$.

The effect of the depth extent

The second factor, containing the variable t can be similarly evaluated. We obtain for $\mathcal{E}\{(1-e^{-2\pi t f_r})\}$ with the uniform distribution

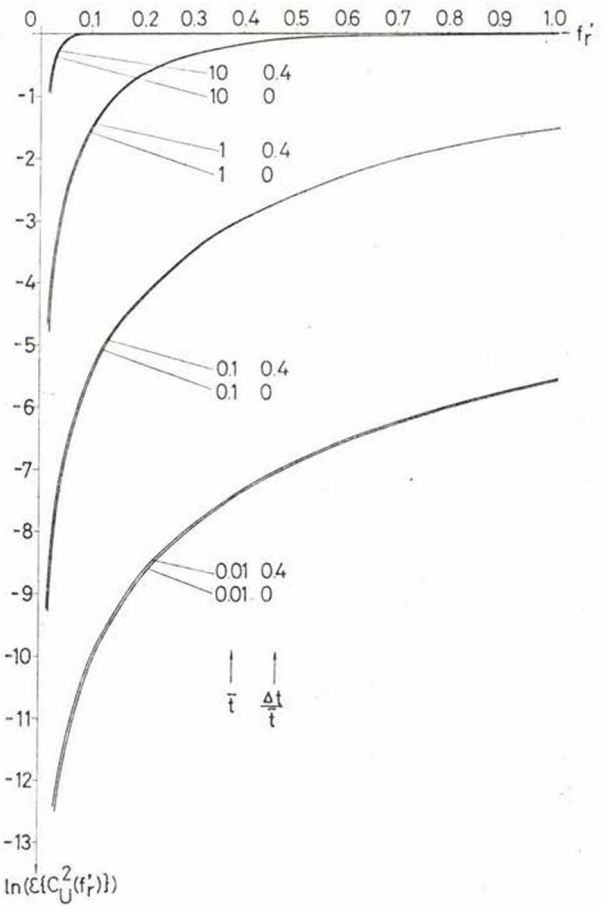

Fig. 13. The expected value of the term describing the effect of depth extent if t follows a uniform distribution with expected value $\bar{t}$ and length Δt

$$\mathcal{E}\{(1-e^{-2\pi t f_r})^2\} \equiv \mathcal{E}\{C_U^2(f_r)\} = \frac{1}{2\Delta t}\int_{\bar{t}+\Delta t}^{\bar{t}-\Delta t}(1-2e^{-2\pi t f_r}+e^{-4\pi t f_r})\,dt =$$

$$= 1-e^{-2\pi \bar{t} f_r}\,\frac{sh(2\pi\,\Delta t f_r)}{\pi \Delta t f_r}+e^{-4\pi \bar{t} f_r}\,\frac{sh(4\pi\,\Delta t f_r)}{4\pi\,\Delta t f_r}\,. \qquad (15)$$

and for the Gaussian distribution

$$\mathcal{E}\{C_G^2(f_r)\} = 1-2e^{-2\pi \bar{t} f_r+2\pi^2\sigma^2 f_r^2}+e^{4\pi \bar{t} f_r+8\pi^2\sigma^2 f_r^2}\,. \qquad (16)$$

The logarithms of the functions (15) and (16) are shown in *Figs. 13 and 14*, respectively.

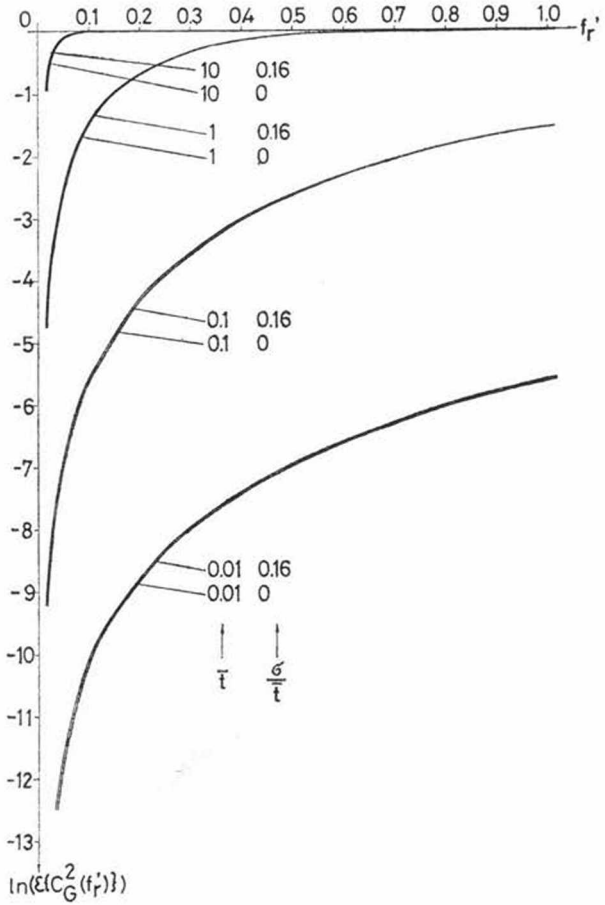

Fig. 14. The expected value of the term describing the effect of depth extent if t follows a uniform distribution with expected value $\bar{t}$ and standard deviation σ

It is worth to note, that the functions describing the depth extent hardly depend on the length of the uniform distribution Δt or on the standard deviation of the Gaussian distribution σ except for very small values of t.

Double ensembles of prismatic bodies

Let us consider last a double ensemble of prismatic bodies. When the parameters h and H (depths to the tops) in the ensembles separates well, and the distributions of the centers of bodies are random without correlation between the two ensembles the expected value of the power spectrum of the magnetic field due to all bodies can be approximated by

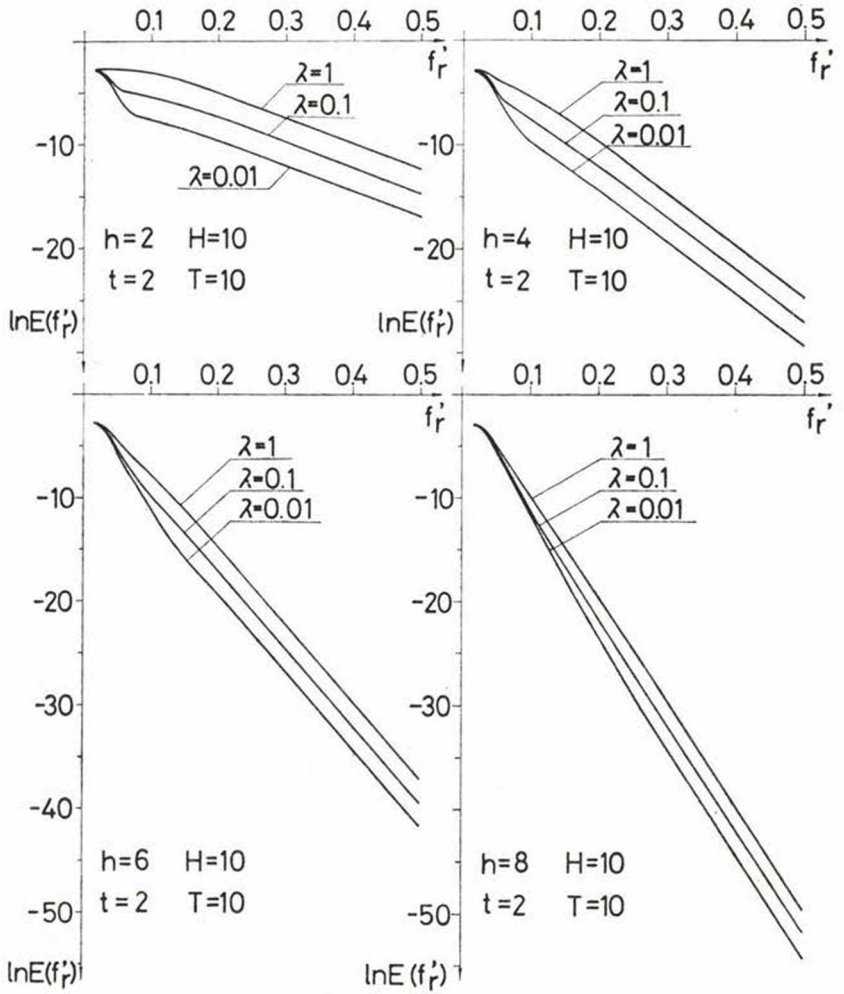

Fig. 15. Logarithmic power spectra for some double ensembles of magnetized bodies. Fixed parameters are: depth extents $T = 10$ (for deeper sources) and $t = 2$ (for shallow sources) and depth of the top of the deeper sources ($H = 10$). The four sets of curves correspond to four different h (depth to top of shallower sources). In each set three energy ratios are shown 1:1, 1:10 and 1:100

$$\mathcal{E}\{E(f_r\ \alpha)\} = 4\pi^2\,\overline{K}^2\mathcal{E}\{e^{-4\pi H f_r}\}\,\mathcal{E}\{(1-e^{-2\pi T f_r})^2\}\,\mathcal{E}\{S_1^2(f_r, d)\} + \\ + 4\pi^2\,\overline{k}^2\mathcal{E}\{e^{-4\pi h f_r}\}\,\mathcal{E}\{(1-e^{-2\pi t f_r})^2\}\,\mathcal{E}\{S_2^2(f_r, \alpha)\} \qquad (17)$$

where K, H, T and k, h, t denotes the expected value of the magnetic moment/unit depth, the depth to the top, the depth extent of the first and the second ensembles of bodies, respectively.

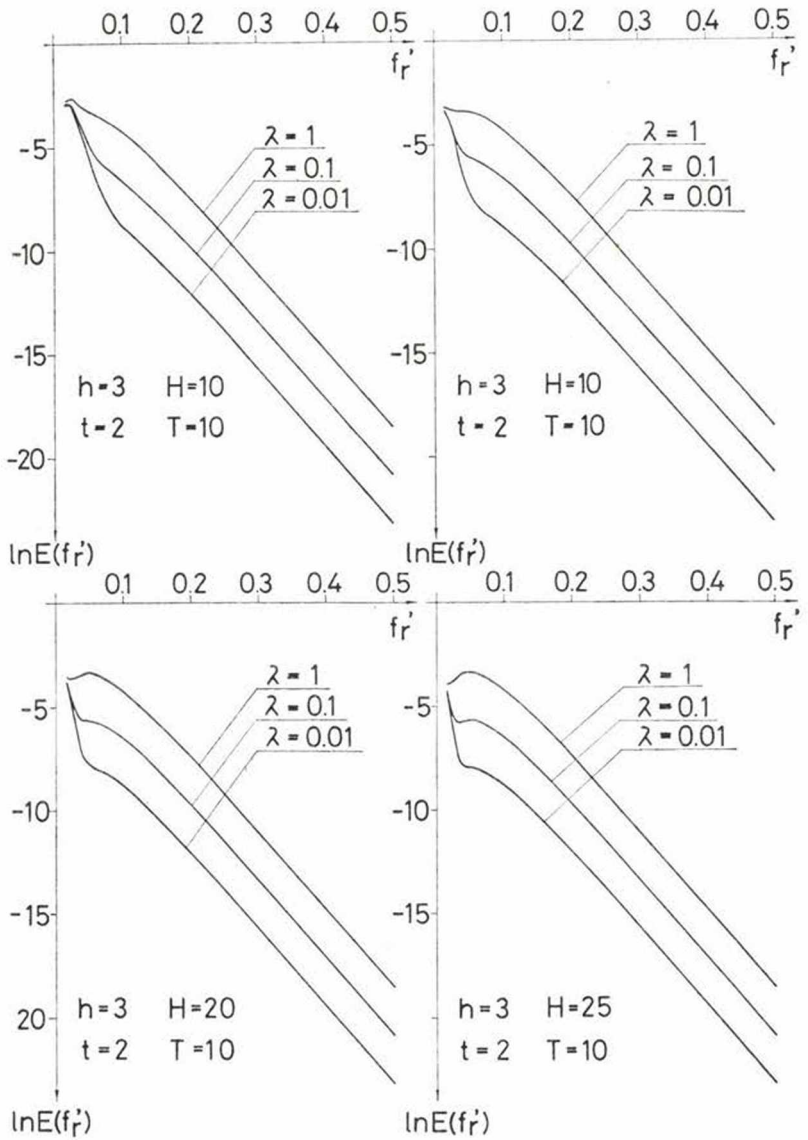

Fig. 16. Logarithmic power spectra for some double ensembles of magnetized bodies. Fixed parameters are: depth extents $T = 10$ (for deeper sources) and $t = 2$ (for shallow sources) and depth of the top of the shallower sources ($h = 3$). The four sets of curves correspond to four different H (depth to top of deeper sources). In each set three energy ratios are shown 1:1, 1:10 and 1:100

$\mathcal{E}\{S_1^2(f_r, a)\}$ and $\mathcal{E}\{S_2^2(f_r a)\}$ contain the effects of the horizontal sizes for the ensembles. In order to get an impression of the behaviour of this rather complicated expression let us assume that $\overline{K}^2 = (\lambda \overline{k})^2\, \mathcal{E}(S_1^2(f_r, \alpha)\} = \mathcal{E}\{S_2^2(f_r, \alpha)\}$ and the parameters H, T, h and t are deterministic. Then (17) simplifies to

$$E_r(f_r) = C[\lambda^2 e^{-4\pi H f_r}(1 - e^{-2\pi T f_r})^2 + e^{-4\pi h f_r}(1 - e^{-2\pi t f_r})^2]. \qquad (18)$$

Figures 15 and 16 show the logarithm of the radial power spectra for some realistic combinations of the parameters λ, H, T, h and t. In *Fig. 15* $H = 10, T = 10, t = 2$ and h varies, while in *Fig. 16* $h = 3, t = 2, T = 10$ and H varies. Both cases are depicted for three different values of the parameter λ.

The most important conclusion which can be drawn from the sets of curves is, that the contribution of the deeper ensemble very rapidly disappears with increasing f_r, i.e. in the estimation of the depth of the deeper sources the first few spectral lines can be used, only. The second conclusion is that t could be determined very rarely and the peak caused by the limited extent of the deeper sources (T) appears at very small frequencies, thus it could be observed very rarely in the spectra of real magnetic data.

REFERENCES

Andreasen, G. E., Zietz, I., 1969: Magnetic fields for 4×6 prismatic model, Geological Survey, Professional Paper 666.

Bhattacharyya, B. K., 1965: Two-dimensional harmonic analysis as a tool for magnetic interpretation, Geophysics, Vol. 30, pp. 829–857.

Bhattacharyya, B. K., 1966: Continuous spectrum of the total magnetic field anomaly due to a rectangular prismatic body, Geophysics, Vol. 31, pp. 97–121.

Bhattacharyya, B. K., 1971: Analysis of a vertical dike, infinitely deep, striking north by Fourier transform, Pure and Applied Geophysics, 89, pp. 134–138.

Bhattacharyya, B. K., Lei-Kuang Leu, 1975: Analysis of magnetic anomalies over Yellowstone National Park: Mapping of Curie point isothermal surface for geothermal reconaissance, Journal of Geophysical Research, Vol. 80, No. 32, pp. 4461–4465.

Cianciara, B., Marcak, H., 1976: Interpretation of gravity anomalies by means of local power spectra, Geophysical Prospecting, Vol. 24, pp. 273–286.

Hahn, A., Kind, E. G., Mishra, D. C., 1976: Depth estimation of magnetic sources by means of Fourier amplitude spectra, Geophysical Prospecting, Vol. 24, pp. 287–308.

Kis, K., Meskó, A., 1977: Application of the Logarithmic Power Spectrum in the Interpretation of Magnetic Data Contributions of the XXII International Geophysical Symp., Prague (in press).

Lehmann, M. J., 1970: Examples for the separation of fields of magnetic sources in different depths by harmonic analysis method, Boll. Geofis. Teor. Appl. 12: 97–117.

Naidu, P. S., 1970: Statistical structure of aeromagnetic field, Geophysics, Vol. 35, pp. 279–292.

Odegard, M. E., Berg, J. W., 1965: Gravity interpretation using the Fourier integral, Geophysics, Vol. 30, pp. 424–438.

Peters, L. J., 1949: The direct approach to magnetic interpretation and its practical application, Geophysics, Vol. 14, 290 – 320.

Sengupta, S., Das, S., 1977: Interpretation of the gravitational effect of two-dimensional dike by Fourier transform, Geoexploration, Vol. 15, pp. 251 – 261.

Spector, A., Bhattacharyya, B. K., 1966: Energy density spectra and autocorrelation functions due to simple magnetic models, Geophysical Prospecting, Vol. 14, pp. 242 – 272.

Spector, A., Grant, F. S., 1970: Statistical models for interpreting aeromagnetic data, Geophysics, Vol. 35, pp. 293 – 302.

Steeland, N. C., 1962: Gravity and Aeromagnetic Exploration in the Paradox Basin, Geophysics, Vol. 17, pp. 73 – 89.

Syberg, F. J. R., 1972: A Fourier method for the regional-residual problem of potential fields, Geophysical Prospecting, Vol. 20, pp. 47 – 75.

Vacquier, V., Steeland, N. C., Henderson, R. G., Zeitz, I., 1971: Interpretation of aeromagnetic maps, Geol. Soc. Am., Memoir, 47.